Plasmon resonance-assisted nanolabels for optical tomography and hyperthermal therapy

Aleksei Smirnov

Institute of Chemistry, St. Petersburg University

G-RISC Project number A-2021 a-2 r, April 29th – May 27th 2021
Principal Investigator Prof. Dr. Eckart Ruehl

Summary

This report is devoted to the synthesis of new plasmonic labels for targeted anti-cancer diagnostics and therapy in the field of transparency of biological tissues (600-800 nm) and the study of interaction with cells by the method of surface-enhanced stimulated Raman scattering.

A new type of gold nanoparticles were synthesized, having a bone-like shape, having an absorption peak in the required region, and without the problems of the presence and the need to separate particles of any other shape in the reaction medium. The nanoparticles were modified with chromophores cyanine 5.5 and 7 and conjugated with folic acid, a delivery vector by various methods: electrostatic immobilization using the technique of layer-by-layer coating with polyelectrolytes with polystyrene sulfonate and polydimethyldiallylammonium, as well as bovine serum albumin, and covalent immobilization - using heterobifunctional amino thiol linkers and activated esters of cyanine and folic acid. The HeLa line was chosen as the folate-positive line, and the HEK Null line as the folate-negative line. It was shown that nanoparticles coated with polyelectrolyte layers are absorbed by HeLa cells and provide an intense signal. Using flow cytometry, it was shown that nanoparticles modified with folic acid are more actively absorbed by HeLa cells than HEK. The MTT test for cytotoxicity in relation to the studied lines allows us to make a preliminary conclusion about the safety of nanoparticles: for concentrations of nanoparticles less than 10 μg/ml, the viability is close to the control group.

These results show promising prospects for further research and clearly indicate the possibility of using this technology in medicine in the future

1. Introduction

A wide range of developments of fluorescent and Raman (Raman) labels based on plasmon signal amplification are presented in some publications of foreign scientific groups and are positioned as potentially suitable for thin-layer ex vivo laboratory studies, as well as for DNA analysis [1]. In any case, their area of action is limited to the middle band of the visible spectrum, outside the red border, so they cannot be used either for three-dimensional mapping of objects deep in biological tissues, or for express analysis during surgical intervention.

To date numerous results on synthetizing of anisotropic nanoparticles of different shape capable of providing the position of the plasmon resonance peak in the 600-800 nm region were presented, which include gold nanoparticles of the rod-shaped family and their derivatives, such as bipyramids, which have already proven themselves as plasmon substrates that provide high signal amplification and the ability to use for bioanalytical and medical purposes [2]–[6]. Colleagues from the University of Washington at St. Louis already used antibody-labeled gold nanorods coated on filter paper to identify cancer biomarkers. Meanwhile El-Sayed et al found that light absorbed by gold nanoparticles is converted into heat in a picosecond interval, which may allow

very point heating when using lasers operating in the appropriate mode [7], [8]. Thus, plasmonic nanoparticles have shown the possibility of using them in hyperthermal point therapy [9], [10]. Much of the radiation absorbed by the nanoparticle is dissipated as heat. Thus, it is possible to carry out a point overheating of cancer cells, leading to their death [11]. However, the research results do not have the ability to determine the location of the particles, and the nanoparticles themselves have low selectivity, and solutions aimed at in vivo diagnostics have not yet been presented.

The present project is dedicated to development of nanocomposite tags for in vitro, ex vivo and in vivo medical diagnostics and therapeutic applications. The resulting nanoparticles modified with chromophores of the cyanine class are coated with a vector of biocompatible compounds of various types and modified delivery with folic acid used for specific binding to folate receptor 1 on the surface of some cancer cells. Polyallylamine hydrochloride can be used in combination with an anionic polyelectrolyte, such as polystyrene sulfonate, to form layer-by-layer adsorbed films of negatively and positively charged polymer [12]. Thus-obtained materials have many biomedical applications [13], [14]. Bovine serum albumin is used to crosslink nanoparticles into agglomerates [12]. It has an isoelectric point of 4.7 and is negatively charged in sodium bicarbonate solution, which allows it to be used to create the next layer after PDDA [15], [16]. Bovine serum albumin is absorbed by cells by itself, and can also be used to mask nanoparticles from phagocytes. Glutaraldehyde, a homobifunctional covalent linker of amino groups, is used as a crosslinking agent. In one of the first studies in 2007, albumin-crosslinked dimers were obtained as agglomerates of spherical gold nanoparticles [17]. The chromophores cyanine 5.5 and cyanine 7 were investigated as fluorescent tags - modifiers of whole silicon oxide nanoparticles [18]. The resulting particles showed high stability in saline as well as in real blood samples. Despite the successful registration of a signal from two fluorophores, the use of silicon particles did not lead to the achievement of a local heating temperature above 43 degrees (under the action of an 808 nm laser), which is necessary for effective cell destruction. The folic acid receptor is a glycoprotein (~ 40 kDa) overexpressed in cancer cells of the body and is involved in the absorption of folic acid - vitamin B9 through a binding mechanism [19]. This receptor exists in two isoforms. FR-α is present in ovarian, brain and kidney carcinoma cells, as well as on some normal epithelial membranes (kidney). Whereas FR-β is present mainly in macrophages and therefore is an ideal receptor for the treatment of inflammatory diseases such as type 2 diabetes, atherosclerosis and rheumatoid arthritis using folate-conjugated nanoparticles containing therapeutic agents. The requirement for precise localization and quantification motivates the development of imaging agents containing positron emitters such as 68Ga [20]. Folic acid receptors are present in normal cells to a lesser extent required for normal functioning [21]. Folic acid prevents DNA changes, and is also responsible for cell growth, metabolism, nucleic acid synthesis, etc. Usually, its deficiency causes anemia of organs such as lungs, breasts, ovaries, colon, kidneys. For comparative studies of folate mediated cellular uptake, the HeLa cell line is generally used as folate positive and HEK293 as folate negative culture [22]–[24].

Stimulated Raman Scattering Spectromicroscopy (SRS) is well-known and precise and widely used for label-free biological studies and mapping of tissues [25]–[28]. Particularly, Stimulated Raman spectroscopy methods is needed to study the distribution and affinity of binding biological labels in matrices and biological tissues and this is the task, the implementation of which is carried out using this method in this work [29], [30].

The ultimate long-term research goal is new nanocomposite labels for *in vitro* and *in vivo* applications. These labels can be used for sensitive tumor localization, metabolic studies, pharmacokinetics of substances, visualization of organ and tumor structures, detection of ultra-

low concentrations of substances in the transparency of biological tissues, as well as plasmon tomography guided surgical manipulations.

2. Materials and Methods

2.1 Materials

Cetyltrimethylammonium bromide (CTAB), HAuCl4 (25 mM stock solution), BSA (bovine serum albumine), HS-PEG-NH_2 Thiol PEG Amine 5000 kDA, N-hydroxysulfosuccinimide, N,N'-Dicyclohexylcarbodiimide, Thioglycolic acid, Cyanine7 amine (Lumiprobe), Cyanine5.5 amine (Lumiprobe), Na_3BH_4, Ascorbic Acid, $AgNO_3$, 4,4'-diaminostilbene (Sigma-Aldrich), 4'4-dimercaptostibene (Sigma-Aldrich), glutaraldehyde, polystyrene sulfonate, polyallylamine ammonium dihydrochloride, cyclen-6, 4,4-diaminebybenzyl, . All dishes were washed with aqua regia prior to use, rinsed with H2O D.I. HeLa and NEK Blue cell lines were obtained from Prof. Dr. Burkhard Kleuser RG (Institute of Pharmacy, Free University of Berlin) and chosen as FOLR1-positive and negative lines correspondingly

2.2 CTAB-stabilized nanoparticles

The synthesis of gold nanoparticles of a new "bone-like" form is based on the procedure for the synthesis of nanorods and differs from the latter in the ratio of the reagents used and the synthesis conditions [31]. General synthesis procedure, calculation for 400 ml of 1x colloid:

Seed solution: 5 ml of CTAB was mixed 5 ml of 0.1 mM HAuCl4, then 0.6 ml of ice-cold $NaBH_4$ was added. The solution goes from pink to cream.

Growth solution: separately 200 ml of CTAB solution was mixed with 10 ml of 10 mM $AgNO_3$ solution under vigorous stirring, then 200 ml of 1 mM $HAuCl_4$ was added. Subsequently 2.8 ml of ascorbic acid was added and 0.552 ml of Seed solution. The solution should be discolored after that. The reaction was stirred for 48 in dark place at 25 C. The final colloid is dark blue.

Washing off excess CTAB is a mandatory step, as after turning off the heating and stirring, the excess CTAB will begin to crystallize. It was shown that if the colloid is then heated again and CTAB dissolved, the plasmon resonance peak is irreversibly changed.

The resulting colloid was centrifuged in 50 ml tubes for 20 minutes at 10,000 rpm. The clear CTAB solution was carefully syphoned off with a dispenser to 0.5 ml of colloid then resuspended with deionized water to its original volume and ulatrasonificated for 30 mins. The colloid was centrifuged one more time in 50 ml tubes for 20 minutes at 8500 rpm, the clear CTAB solution was syphoned off with a dispenser to 0.5 ml of colloid, then colloid was resuspended with deionized water to the desired volume. Resulting colloid was ultrasonificated for 30 mins prior to subsequent use.

2.3 Core-shell folic acid conjugated nanoparticles

The scheme of coating with layers of polyelectrolytes was created and optimized experimentally and on the basis of a number of literature sources describing similar methods [32]–[37]: 100 ml of the purified colloid was added dropwise with stirring to 100 ml of a solution containing 2 g/L PSS, 6 mM NaCl and left stirring until the next day (Figure 1). The resulting 200 ml were purified by centrifugation at 8500 rpm, 50 ml in 50 ml tubes and resuspended from 0.5 ml to 20. The tubes were kept in an ultrasonic bath for 30 minutes, after which the colloid was combined and brought to the original 100 ml. Chromophores were added dropwise at this stage as 10^{-4} M solutions and left under vigorous stirring for 2 hours. 1 volume of the resulting colloid was added dropwise with stirring to 1 volume of a solution containing 2 g/L of PDDA and left stirring

until the next day. The resulting colloid were purified by centrifugation at 7500 rpm, 50 ml in 50 ml tubes and resuspended from 0.5 ml to 20. The tubes were kept in an ultrasonic bath for 30 minutes, after which the colloid was combined and brought to the original volume.

Folic acid (FA) as a low molecular weight vector was selected as model vector for evaluating anti-tumor applicability of approach. 10^{-4} M solution of FA in 0.1 M $NaHCO_3$. In systems where modification with folic acid was carried out electrostatically (due to the coating of nanoparticles with a layer of polycationite - PDDA) folic acid at a concentration of 10^{-4} M, dissolved in a bicarbonate buffer, was added dropwise with stirring to a single solution of nanoparticles in a 1:1 ratio, thus reaching a final concentration of $5*10^{-5}$ M, the system was incubated for 2 hours with stirring, after which the excess folic acid was removed by centrifugation (Figure 1). Prior to conjugate the vector of nanoparticles, functionalized with amino groups by incubation with Thiol PEG Amine NHS-activated ester of folic acid was obtained (see Supplementary materials). Before this step nanoparticles were modified with cysteamine and then with commercially available NHS-activated ester of cyanine 5.5 (Figure 2).

In the case of systems with bovine serum albumin layer placed after PDDA by incubation with 10 g/L in the same way as was described for other polyelectrolyte layers activated ester of folic acid was also used. The excess of surface modifiers was removed by centrifugation after each described step.

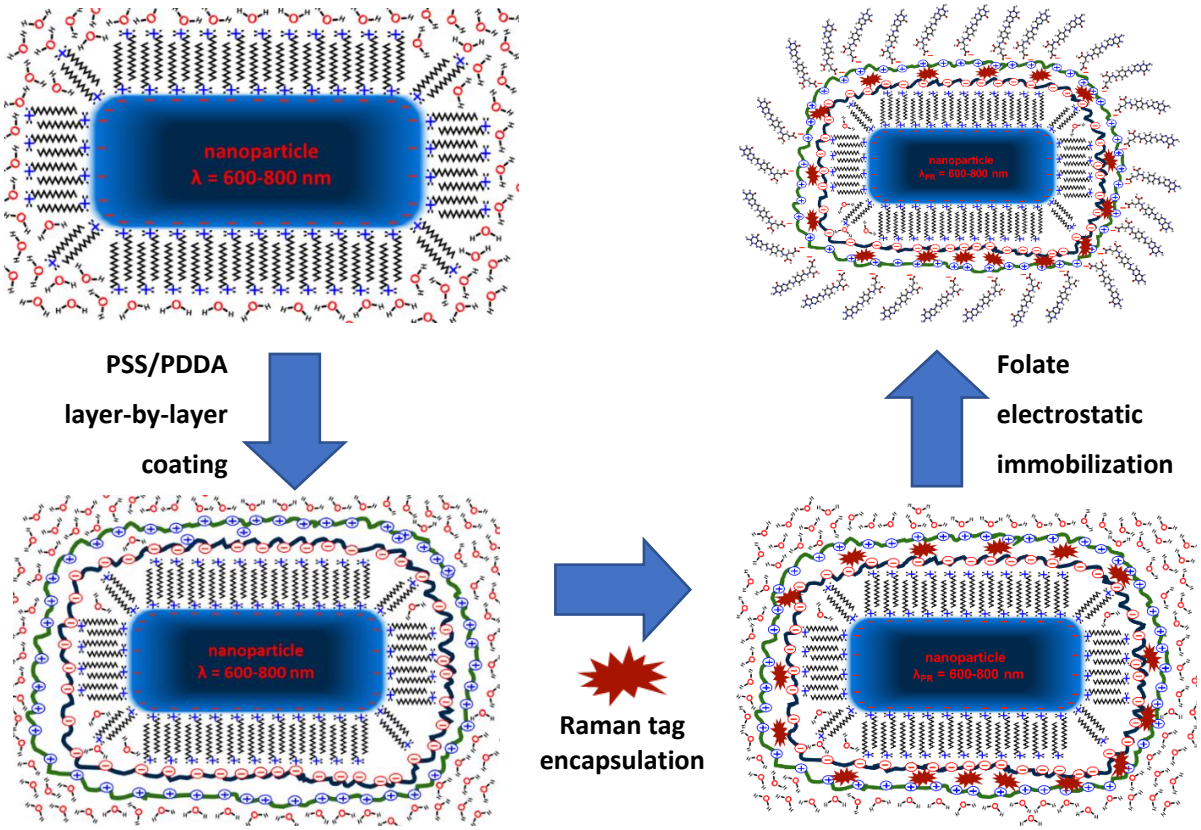

Figure 1. Schematic representation of polyelectrolyte layer-by-layer coating of CTAB-stabilized gold nanoparticles with electrostatic encapsulation of charged chromophore and folate vector immobilization.

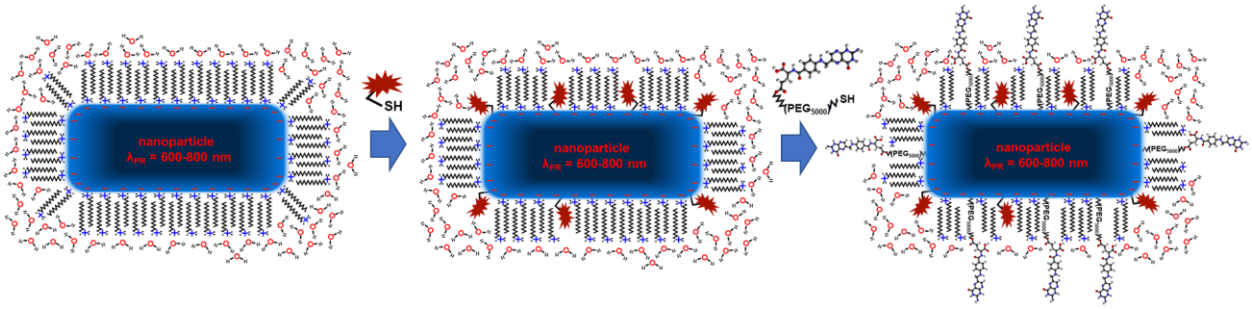

Figure 2. Schematic representation of covalent immobilization of CTAB-stabilized gold nanoparticles with thiol-modified chromophore and folic acid.

3. Methods

Describe in 200-500 words the experimental and/or theoretical methods used in the project.

3.1 Methods of spectrometry used for characterization of synthetized nanoparticles

The recording of electronic spectra of colloidal solutions of nanoparticles was carried out in the range of 190-1100 nm on scanning spectrometers UV-1800 and UV-2550 in quartz cells with an optical path length of 10 mm.

Dynamic Light Scattering study was performed with refractive index 0.27 and index 5.95 were used as preset in the device. The viscosity of the solvent is set as for water equal to 0.887 Pa * with a refractive index equal to 1.33.

^{13}C NMR spectra of folic acid and its activated ester were obtained on a Bruker 400 MHz Avance instrument. This type of spectroscopy was used to confirm the activation of the terminal carboxyl group of folic acid by n-hydroxysuccinimide, the operating frequency is 100.623 MHz.

3.2 Preparation of cell samples

For Stimulated Raman Spectromicroscopy and Flow Cytometry studies cell lines were incubated overnight in the 6-well plates filled with cover slips at $0.3*10^6$ seeding density in standard growth media (DMEM with 10% FBS, glutamine, streptomycin, amphotericin B, penicillin). Afterwards media was syphoned out, units were washed with PBS and filled with 2 ml FBS-deficient growth media (1% FBS) containing 3 ug/ml of nanoparticles in 3 biological replicates and control samples without nanoparticles. After 2- or 24-hours incubation, cells were washed twice with PBS, coverslips were transferred to new 6-well plates and fixed with 4% formaldehyde in PBS for 15 minutes, then washed again with PBS. The cover slips were removed and sealed around the perimeter with epoxy resin on glass slides to avoid buffer evaporation and allow for long-term storage. The cells remaining in the wells of the original plates (in which the incubation was carried out) were treated with trypsin and used for studies using flow cytometry.

The MTT test is a general test that allows the cumulative assessment of cell viability under the influence of the test objects. NAD(P)H-dependent cellular oxidoreductase enzymes reduce the tetrazolium dye MTT 3-(4,5-dimethylthiazol-2-yl)-2,5-diphenyltetrazolium bromide, which has yellow color in water solutions to its insoluble formazan, which has a purple color (540 nm absorbance wavelength is usually used for measurements). HeLa, which is widely used as folate-positive line was selected for the test [38]. A 96-well plate was seeded with HeLa cells with 10000 cells/unit density and incubated with standard growth media (DMEM with 10% FBS, glutamine, streptomycin, amphotericin B, penicillin) overnight. [39]. After that, medium was syphoned out and units were filled with standard growth media with 0.01 , 0.1 , 1 and 10 ug/ml concentration of

nanoparticles in 5 biological replicates. Cell viability was studied for 3 different types of nanoparticles (details may be found in the Results section), 16 units were used for untreated control cells (Figure 7).

3.3 Spontaneous Surface Enhanced Raman Spectroscopy

The recording of the Surface Enhanced Raman Scattering spectra was carried out on a LabRam HR 800 spectrometer and a SENTERRA express Raman spectrometer (Bruker) in reflection geometry setup using a modified optical microscope (BX41, Olympus) equipped with 40x standard objective (MPLN, Olympus) Excitation line was 632.8 nm at 30 mW. All studies are carried out in 10 mm quartz cuvettes for 2 and 3 ml. Accumulation time was 16 s, number of accumulations 10 in 4 repeats. The measurements was carried out in the range 100-1800 cm-1 with a fiber-coupled 80 cm Jobin Yvon spectrometer (Dilor triple XY 800, Horiba) using three 600 l/mm gratings in the subtractive mode. Raman spectra were taken each point two times. 1.5 ml Eppendorf tubes were filled to the neck with undiluted colloidal solutions of nanoparticles (approximately 106 ug/ml) and closed with cover glass to cope with surface curvature of the liquid and prevent evaporation during measurements. The laser focusing was set on the lower boundary of the cover glass, and then shifted 1 mm downward along the z axis to obtain a signal. The signal for cell preparations was obtained by focusing 5 μm below the lower edge of the coverslip in the central part of the HeLa cell.

3.4 Quantum chemical simulation

To allow an approximate assignment of the main vibrational modes for cyanine 5 amine, quantum-chemical calculations of their vibrational modes were carried out using the hybrid functional b3lyp in the 3-21g basis set. Quantum-chemical calculations were performed using the Gaussian-16 software package [40] under license from St. Petersburg State University on the computing cluster of the Computing Center resource center of St. Petersburg State University. The calculations began with the optimization of the conformation of the molecule, set manually and presumably the closest to the real one from the considerations of the calculated experience and literature data for close compounds. For comparison with experiment, all fundamental vibrational frequencies calculated using the GaussView program were multiplied by a factor of 0.97 97 [41], [42].

3.5 Stimulated Surface Enhanced Raman Spectromicroscopy

Stimulated Raman Spectroicroscopy (SRS) studies were performed using an IX83 Olympus microscope, equipped with a 50x NIR objective (LCPLN50XIR, Olympus). The samples were excited by a PicoEmerald laser system (APE, Berlin), with a pulse width of 6 ps and a repetition rate of 80 MHz. This laser emits two pulses, where one was kept at fixed wavelength (Stokes pulse, 1064.2 nm). The wavelength of the preceding pump pulse was adjusted according to the desired Raman transition using the signal wave of the optical parametric oscillator (OPO). For these studies we have chosen several most pronounced Raman modes according to the results of spontaneous surface enhanced Raman spectrometry studies of nanoparticles in colloid solutions, which are not overlap with signal from cells (Figure 6, Results section). To check reliability of signal we also performed the mapping at 2930 cm^{-1} wavenumber, which corresponds to the Raman scattering from proteins.

Measuring the SRS process was realized in Stimulated Raman-Loss (SRL) detection technique. The Stokes beam was modulated by an electrooptical modulator (EOM) to 20 MHz. Modulations of the transmitted pump beam were detected by a fast photo diode (DET36A, Thorlabs) and a lock-in amplifier (HF2TA + HF2LI Zurich Instruments).

In order to avoid radiation damage of the samples the laser power was limited to 5 mW and 12.5 mW for pump- and Stokes-beam, respectively. Stimulated Raman maps were performed by scanning the microscope stage with a dwell time at one spot of 160 ms. Possible unwanted backgrounds from cross-phase modulation or other effects are reduced by subtracting background maps performed at 2500 cm^{-1} , corresponding to a pump beam wavelength of 840.6 nm, where no Raman signal is emitted from skin samples.

4. Results and Discussion

4.1 TEM microphotographs of nanoparticles

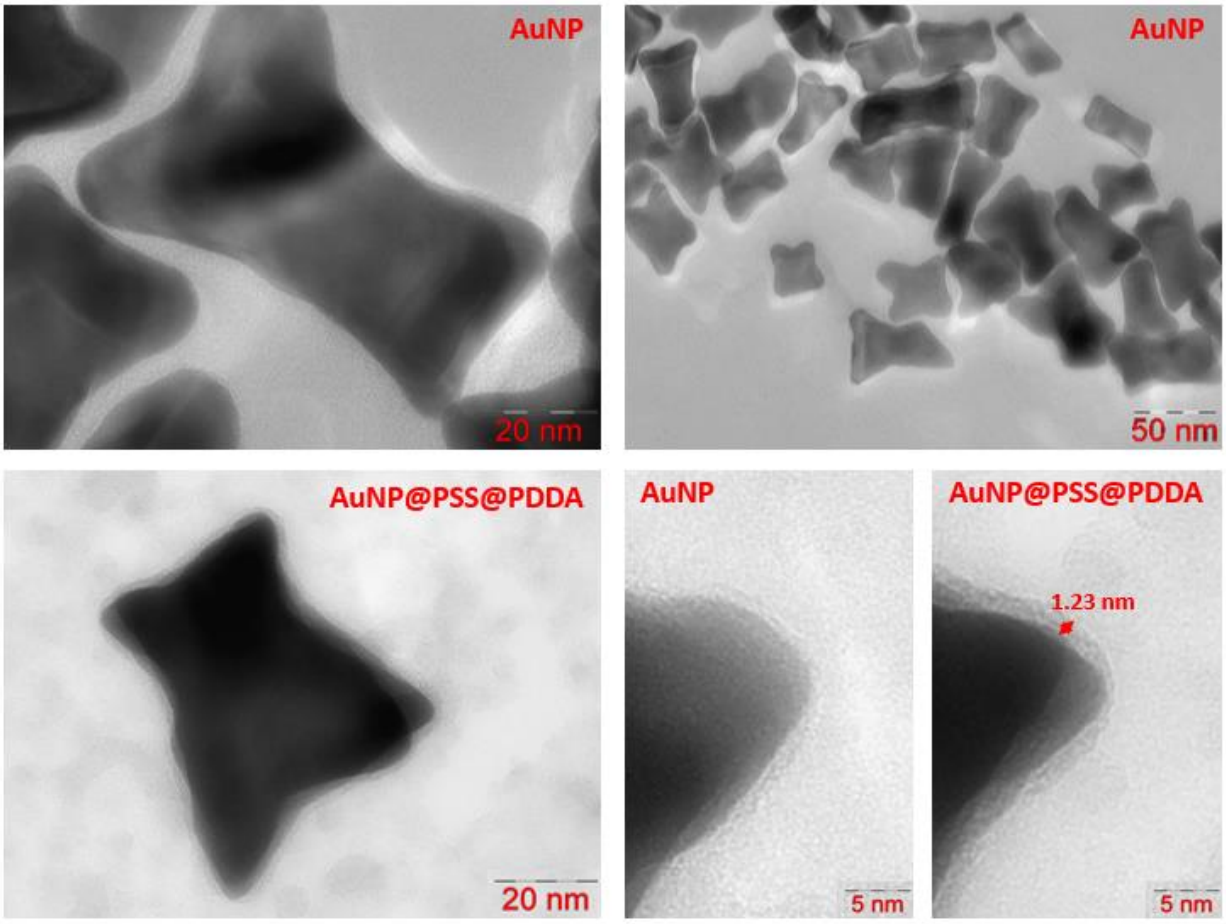

Figure 3. TEM images of CTAB-stabilized bone nanoparticles used in this study, as well as particles coated with PSS and PDDA layers.

One can immediately note the advantage of the new method - as a result of synthesis, only target particles are formed (with absorption in the 600-800 nm region, Supplementary materials, Figure S1). According to the original method for the synthesis of gold bipyramids, as can be seen from the obtained TEM images, spherical particles with absorption in the 530 nm region are also formed, which are undesirable (Figure 3). At the same time, their separation is a rather difficult, resource-intensive and ineffective process. The new method also uses silver nitrate in addition to gold hydrogen tetrachloroaurate. Accordingly, it is correct to call these particles bimetallic, because silver also participates in the construction of the crystal lattice of nanoparticles. Due to a more diffuse plasmon peak, which allows measurements both in the 632.8 nm region and in the 785 nm region, reproducibility of synthesis, reproducible working methods of coating, as well as the

absence of spherical particles, it was further decided to investigate these new bone-shaped particles.

4.2 Spontaneous Raman measurements

Alongside with cyanine 5.5 and 7 dyes several another known and well-studied chromophores were tested as potential promising Raman tags: 4,4'-diaminostilbene, 4'4-dimercaptostibene, cyclen-6, 4,4-diaminebybenzyl. For these nanoparticles bovine serum albumin cross-linked by glutaraldehyde have been chosen. Cross-linking is used to obtain dense ad durable shell, dimers and agglomerates of nanoparticles [43], [44]. Spontaneous Raman scattering study revealed, that cross-linking lead to high fluorescence signal even at 632.8 excitation wavelength and makes it impossible to use such systems as Raman tags. In 2016 it was that the cross-linking of BSA molecules by themselves can significantly affect the optical properties of the cross-linked protein and such BSA hydrogels had fluorescence in the green region of the spectrum [45].

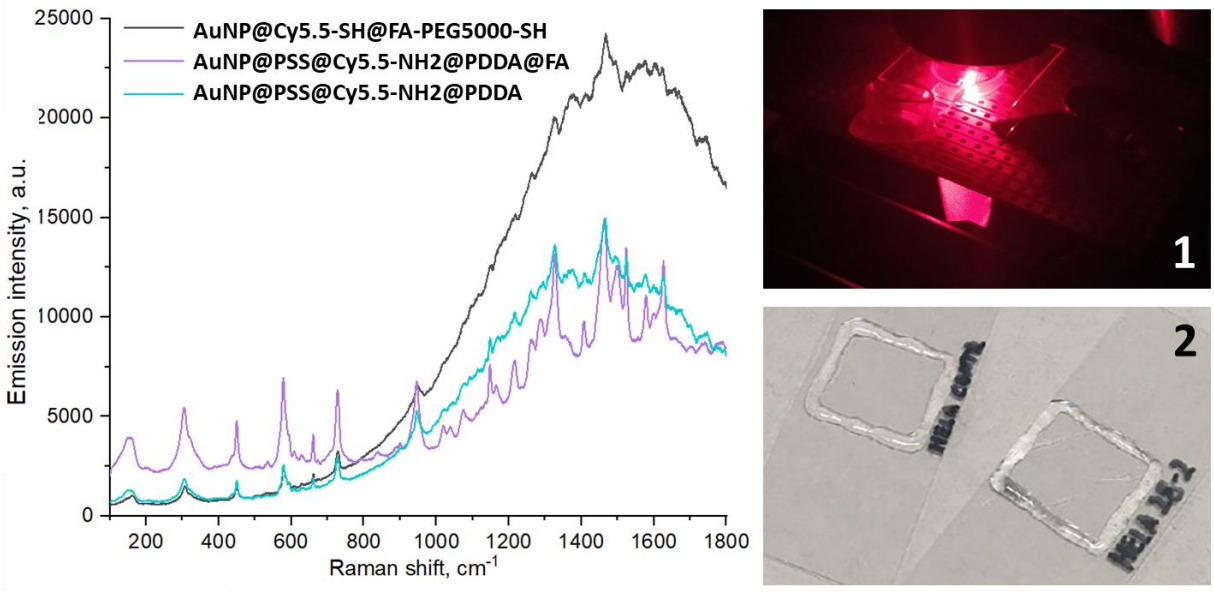

Figure 4. Surface enhanced Raman scattering spectra of systems, which were chosen for SRS studies. Photograph 1 shows setup for spontaneous Raman scattering spectra registration, Photograph 2 shows cell samples after treatment with nanoparticles and sealing with epoxy glue.

We have chosen 1 - AuNP@PSS@Cy5.5-NH2@PDDA@FA ; 2 - AuNP@PSS@Cy5.5-NH2@PDDA ; 3 - AuNP@Cy5.5-SH@FA-PEG5000-SH ; 4 - AuNP@Cy5.5-NH2@PDDA@BSA-FA ; 5 - AuNP@Cy7 -NH2@PDDA@BSA-FA nanoparticles as the most promising systems for the following cell studies.

The first two types of nanoparticles differ only in the presence or absence of electrostatically immobilized folic acid on the surface of the nanoparticle surface. Studies of dynamic light scattering on these particles, covered with a layer of PSS, and then PDDA and washed from excess polymer showed a zeta potential value of +42±2 mV (3 repeats of measurement). Immobilization on a positively charged surface of a polycationite of folic acid dissolved in an alkaline buffer (sodium bicarbonate) is carried out at the terminal caraboxyl. In one of the studies, folic acid was co-crystallized with the folic acid receptor 1 and it was shown that the terminal carboxyl group does not participate in the interaction with the receptor, remains sterically uncomplicated, and can be used to conjugate objects that need to be delivered to cells. This comparative study should show the role of folic acid in these systems.

The third type of nanoparticles carries a fundamentally different idea of surface modification: covalent immobilization of the chromophore using a short linker (cysteamine - to quench near-surface fluorescence and obtain the SERS signal) on the gold surface using a thiol group, and folic acid using a long (5 kDa PEG) linker to minimize possible steric hindrance when interacting with the receptor.

The fourth and fifth samples differ from the first by the presence of a layer of bovine serum albumin, to which folic acid is covalently conjugated (in the form of a previously isolated NHS-activated folic acid ester, see Supplementary Materials). The fourth and fifth samples differ in the chromophore used: when creating the fifth sample, cyanine 7 was used, which in its pure form has absorption and emission in the redder region, instead of cyanine 5.5

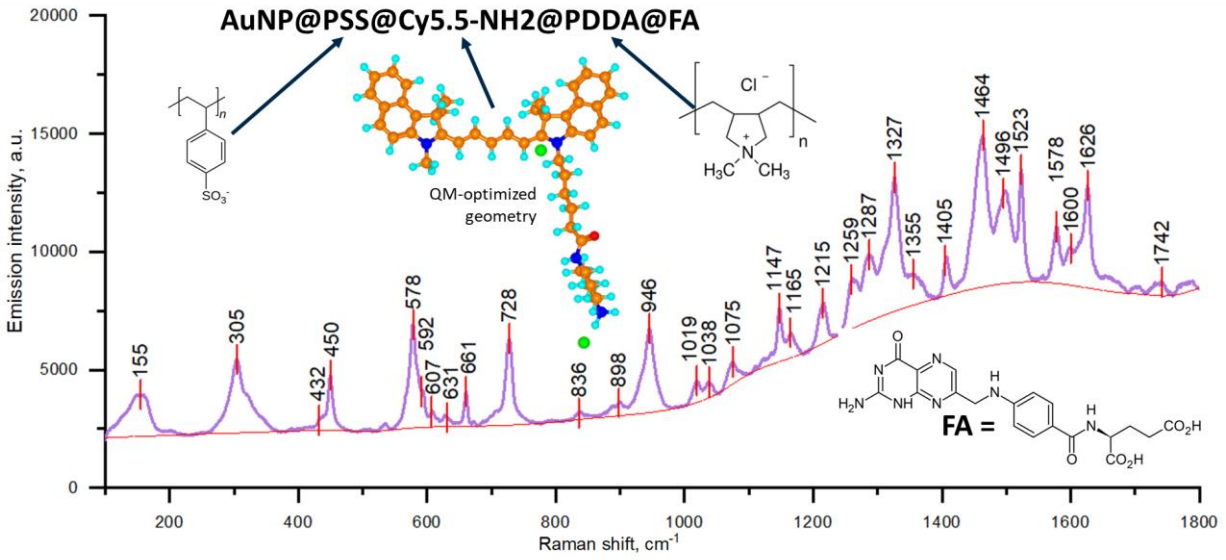

Figure 5. Surface Enhanced Raman spectra of core-shell Cyanine 5.5-amine modified nanoparticles, modified with folic acid. Assignment of the most major modes may be found at Fig. S` (Supplementary materials)

When choosing the wave numbers for tuning the pump laser, we were guided not only by the most pronounced vibrational modes based on the results of CEPC registration of colloidal solutions of the corresponding nanoparticles, but also by the laser modulation range, as well as by excluding interference with the vibrational transitions of the cell culture itself (Figure 5,6). 1326 cm^{-1} and 1148 cm^{-1} wavenumbers turned out to be the most suitable; according to the results of quantum-chemical modeling, the first was attributed to the deformational CH vibrations of the cyanine 5.5 amine molecule, the second also includes stretching vibrations of the carbon backbone (Figure S1, Supplementary Materials). Wavenumber 1460 cm^{-1} (NC-H3 deformational) had high intensity, but unfortunately it interferes with HeLa cells Raman signal and thus can't be used (Figure 6).

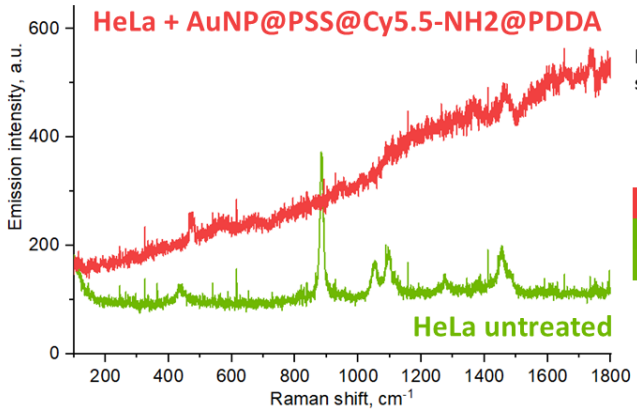

Raman shift, cm^{-1}	Probe Wavelength, nm	Ex. Line, nm	
1626	1064	907.1	
1578	1064	911.0	
1523	1064	915.6	
1460	**1064**	**920.9**	interference with HeLa
1326	**1064**	**932.4**	
1148	**1064**	**948.2**	
1074	1064	954.9	
945	**1064**	**966.8**	
727	**1064**	**987.6**	

Figure 6. Left: Raman spectra of HeLa cells samples after 2 hours of treatment with nanoparticles (Red spectra) and untreated cells (Green spectra). Right: Major wavenumbers, which were chosen as the most appropriate for SRS study according to preliminary spontaneous Raman study (Figure 5).

4.4 Flow Cytometry Scattering measurements

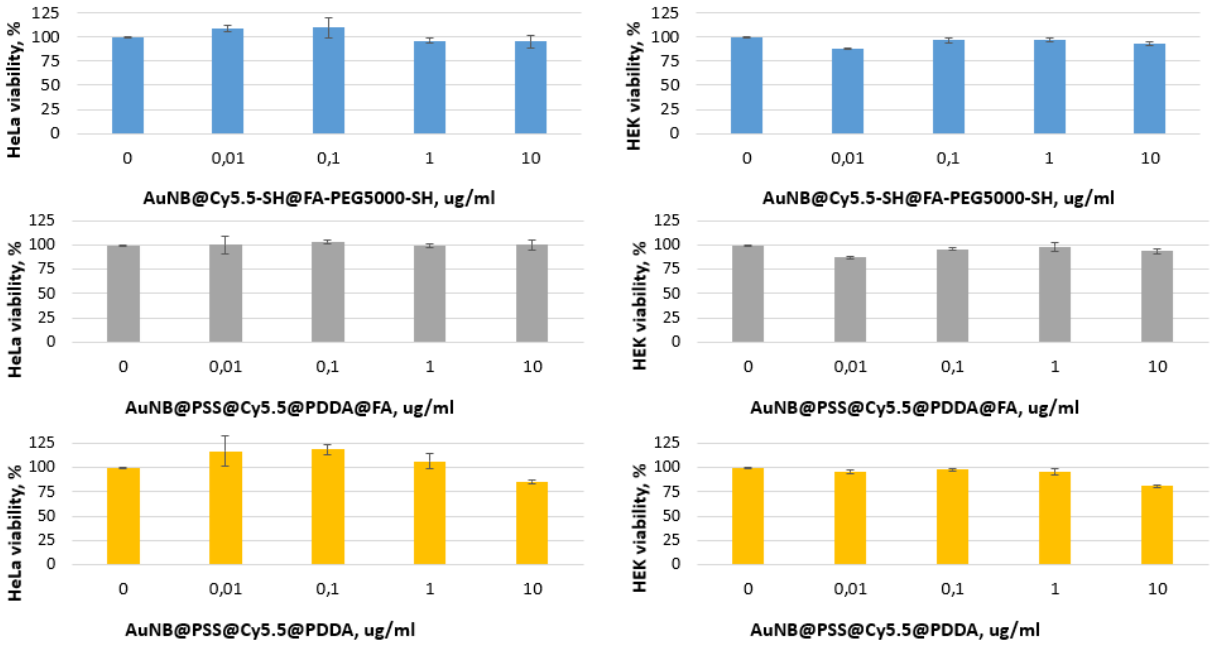

Figure 5. HeLa and HEK viability tests (MTT) in the presence of different nanoparticles, exposure time: 24 hours

The viability test showed a comparative lack of cytotoxicity of nanoparticles in relation both to the HeLa and HEK cell lines (Figure 5). Thus, the studied nanoparticles can be preliminarily considered safe for *in vivo* use. Viability higher than 100% in case of small concentrations of nanoparticles means, that these nanoparticles induce cell proliferation and cannot be easily explained, because AuNP@PSS@Cy5.5@PDDA is not conjugated with folic acid and thus does not contain obvious components that could be involved in cellular metabolism. The same particles exhibit cytotoxicity, reducing cell viability to 80% in the case of a maximum concentration of 10 μg/ml, which is still considered a rather weak effect [46].

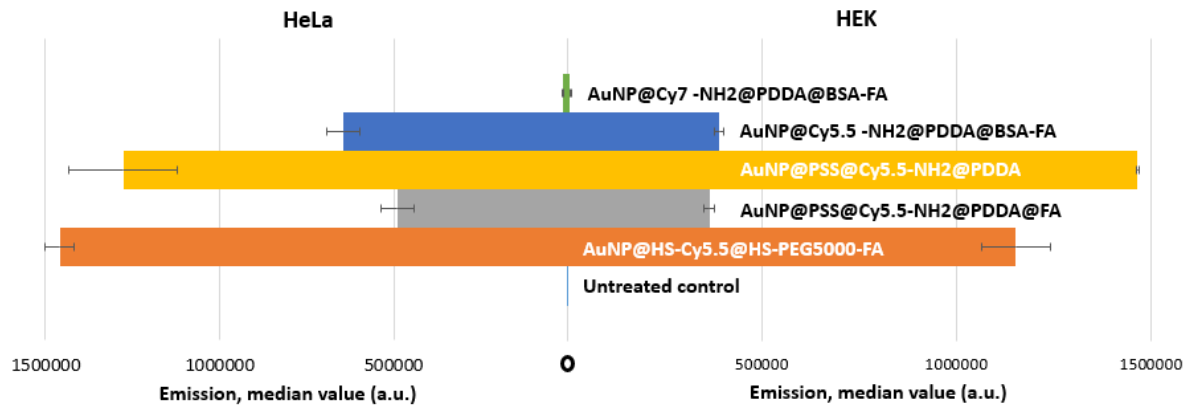

Figure 7. Flow cytometry measurement of fluorescent signal of cells recorded at a wavelength of 712 nm and integrated over the registration window area of 25 nm, excitation line at 638 nm. The values represent median signal of values selected by side and forward violet scattering (Fig. S2, Supplementary Materials), the mean over 3 biological replicates. Exposure time of nanoparticles: 24 hours.

Flow cytometry was used as an experiment to preliminary estimate the optical response of cells exposed to the action of nanoparticles. (Fig. 7). Almost the same flow cytometry results were obtained when incubated for 24 hours between folate-positive and folate-negative cell lines. Perhaps, during this time, a balance between the number of nanoparticles in the medium and inside the cells has been established, so it was decided to repeat the test with incubation for 2 hours (Fig. 8). Meanwhile, we found more intense scattering from cells incubated with PDDA-coated nanoparticles without folic acid versus nanoparticles modified with folic acid. Particles in which cyanine 7 was used instead of cyanine 5.5 showed weak emission against the background of other particles, however, more than in the case of the control sample (Figure 7)

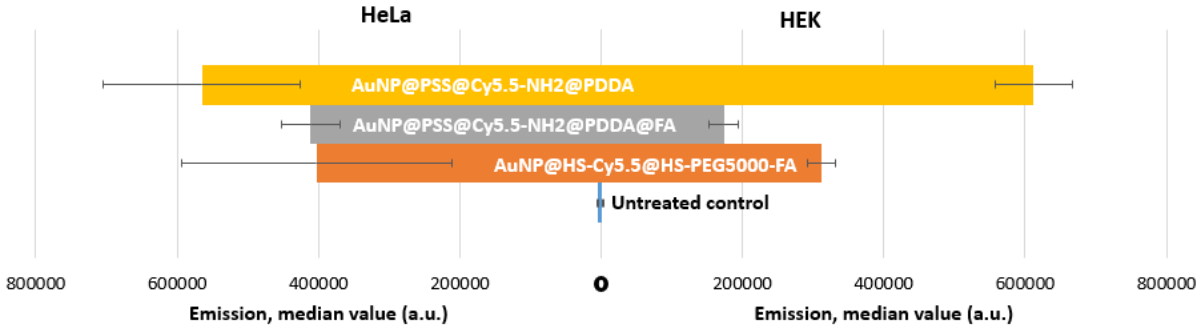

Figure 8. Flow cytometry measurement of fluorescent signal of cells recorded at a wavelength of 660 nm and integrated over the registration window area of 10 nm, excitation line at 638 nm. The values represent median signal of values selected by side and forward violet scattering (Fig. S2, Supplementary Materials), the mean over 3 biological replicates. Exposure time of nanoparticles: 24 hours.

By comparing the results obtained for samples incubated for 24 and 2 hours, a folic acid conjugated sample can be isolated. The difference between folate positive lines and folate negative lines can be traced for this type of nanoparticle, while for particles of the same type, not conjugated with folic acid, there is no such difference. Apparently, nanoparticles not modified with folic acid

undergo strong passive endocytosis from the side of cells and this mechanism is not associated with the level of expression of folate receptors.

In the case of the same particles modified with folic acid, the latter partially screens the surface charge created by the amino groups of the polycation exchanger, and the contribution of folate receptors to the degree of binding of nanoparticles to cells becomes more pronounced and different for two cell lines.

4.4 Stimulated Raman spectromicroscopy

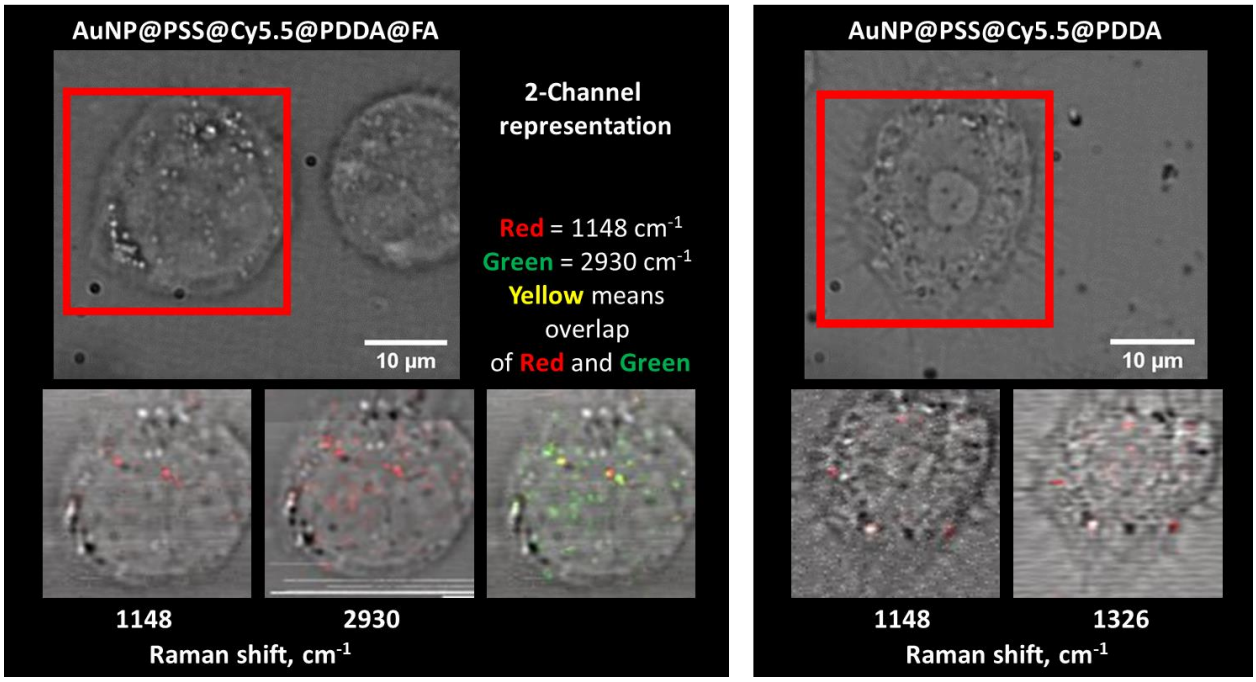

Figure 9. Stimulated Surface Enhanced Raman Scattering mapping

Stimulated Raman signal from protein located at the same place as Raman signal form nanoparticles prove the presence of nanoparticles by its ability to enhance Raman signal of surrounding biomolecules (Figure 9) [47]–[49]. The presence of an enhancement of the protein signal also proves that the nanoparticles penetrated into the cells, and were not immobilized on their surface.

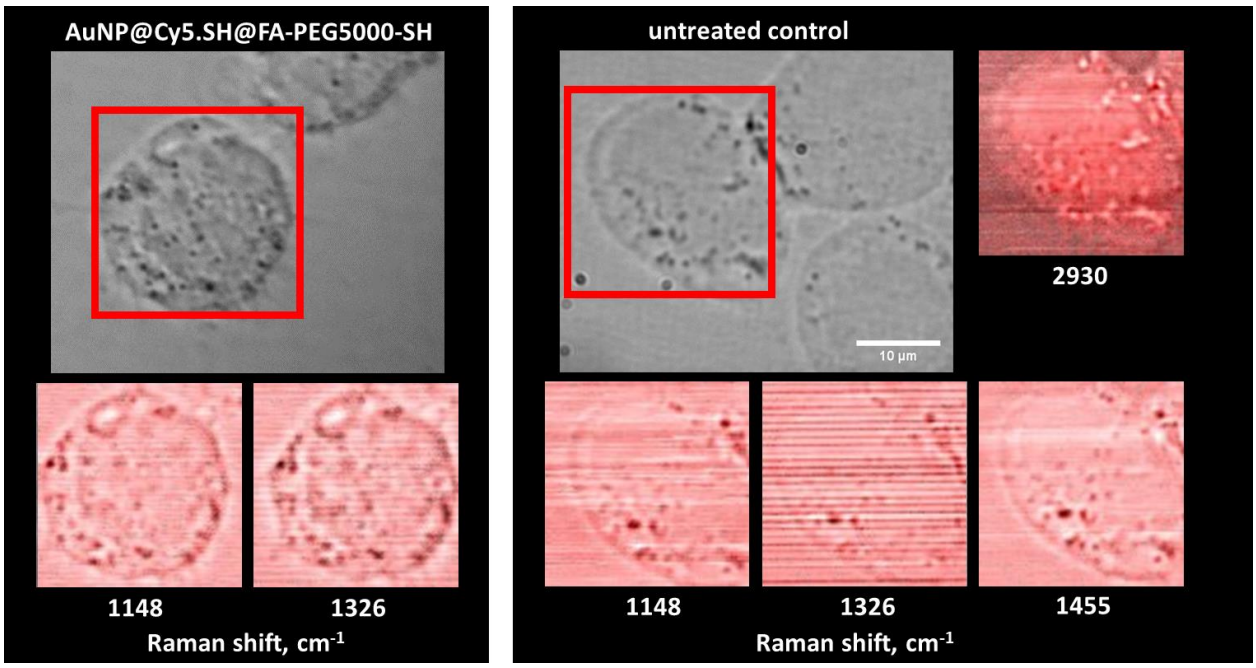

Figure 10. Stimulated Surface Enhanced Raman Scattering mapping

At similar wavelengths, the control sample (HeLa cells not exposed to any nanoparticles) and the sample in which the chromophore and folic acid were covalently immobilized did not show any scattering (Figure 10). The uniform color distribution in Figure 10 corresponds to the background signal level.

5. Conclusion

A technique has been developed for the synthesis of gold nanoparticles of a new bone-like shape with a plasmon resonance absorption band in the region of 600-800 nm. Bone-shaped gold nanoparticles were selected as optimal objects for further modification and attachment of delivery vectors. Methods for coating gold nanoparticles of bone-like shape with layers of polyelectrolytes, bovine serum albumin and direct covalent modification were studied and compared on biological samples. The modification of bone-shaped gold nanoparticles was carried out with two chromophores: cyanine 5.5 amine and cyanine 7 amine. The possibility of using modified nanoparticles as fluorescent and SRS labels is shown. The study and assignment of the Raman spectra of cyanine 5.5 amine. Testing of gold nanoparticles of bone form, conjugated with folic acid, on the line of cancer cells HeLa and HEK, studied the effect of the nature of the surface of nanoparticles on cytotoxicity. Model nanoparticles have been tested for cytotoxicity against cancer cell line HeLa utilizing

The results of the work prove the promising of the transition to extended cell tests and the development of photothermal methods. Already in the objective future, in this work, labels based on the effect of plasmon resonance can become a new development for solving problems of medical diagnostics of malignant neoplasms. The work is interdisciplinary, as it combines the use of new principles, extensive chemical synthesis, research on biological objects. Distinctive features of the proposed approach are signal intensity, minimization of the interfering contribution to the signal from natural and scattered human tissues, biocompatibility, and the use of metal nanoparticles, which is promising for photothermal therapy along with diagnostics.

Further studies will include mapping HEK cells, selected as a control folate-negative line in the laboratory of the Free University of Berlin, as well as accurate quantitative analysis of the

absorption of nanoparticles by cells using atomic emission spectrometry in inductively coupled plasma at the resource center of St. Petersburg State University. The results of the work are planned to be included in the publication in a peer-reviewed journal and also presented as a report at the conference.

6. References

[1] N. Banaei, A. Foley, J. M. Houghton, Y. Sun, and B. Kim, *Nanotechnology*, 28, 45, (2017),

[2] G. Uchehara, A. G. Kirk, M. Trifiro, M. Paliouras, and P. Mohammadyousef, in *Nano-, Bio-, Info-Tech Sensors and 3D Systems III*, Mar. 2019, 10969, 9. doi: 10.1117/12.2518295.

[3] S. K. Panda, S. Chakraborti, and R. N. Basu, *Bull. Mater. Sci.*, 41, 4, 1–7, (2018),

[4] Z. Q. Tian, B. Ren, and D. Y. Wu, *Journal of Physical Chemistry B*, 106, 37. 9463–9483, Sep. 19, 2002. doi: 10.1021/jp0257449.

[5] B. K. Sahu, A. Dwivedi, K. K. Pal, R. Pandian, S. Dhara, and A. Das, *Appl. Surf. Sci.*, 537, (2021),

[6] N. D. Burrows, S. Harvey, F. A. Idesis, and C. J. Murphy, *Langmuir*, 33, 8, 1891–1907, (2017),

[7] S. Link and M. A. El-Sayed, *International Reviews in Physical Chemistry*, 19, 3. Taylor & Francis Group , 409–453, 2000. doi: 10.1080/01442350050034180.

[8] S. Link and M. A. El-Sayed, *Annual Review of Physical Chemistry*, 54, 1. 331–366, Oct. 2003. doi: 10.1146/annurev.physchem.54.011002.103759.

[9] A. S. Lapchenko, *Vestnik otorinolaringologii*, 80, 6. Издательство “Медиа Сфера,” 4–9, 2015. doi: 10.17116/otorino20158064-9.

[10] E. M. Schuh, R. Portela, H. L. Gardner, C. Schoen, and C. A. London, *BMC Vet. Res.*, 13, 1, 294, (2017),

[11] J. Beik *et al.*, *Journal of Controlled Release*, 235. Elsevier B.V., 205–221, Aug. 10, 2016. doi: 10.1016/j.jconrel.2016.05.062.

[12] R. P. M. Höller *et al.*, *ACS Appl. Mater. Interfaces*, 12, 51, 57302–57313, (2020),

[13] J. Kim *et al.*, *Nano Lett.*, 15, 8, 5574–5579, (2015),

[14] O. H. Shayesteh and R. Ghavami, *Spectrochim. Acta - Part A Mol. Biomol. Spectrosc.*, 226, (2020),

[15] I. Matei, C. M. Buta, I. M. Turcu, D. Culita, C. Munteanu, and G. Ionita, *Molecules*, 24, 18, (2019),

[16] E. S. Bronze-Uhle, B. C. Costa, V. F. Ximenes, and P. N. Lisboa-Filho, *Nanotechnol. Sci. Appl.*, 10, 11–21, (2017),

[17] L. Sun *et al.*, *Nano Lett.*, 7, 2, 351–356, (2007),

[18] S. Biffi *et al.*, *Int. J. Nanomedicine*, 11, 4865–4874, (2016),

[19] I. Nallamuthu, F. Khanum, S. J. Fathima, M. M. Patil, and T. Anand, in *Nutrient Delivery*, Elsevier, 2017, 619–651. doi: 10.1016/b978-0-12-804304-2.00016-0.

[20] I. Velikyan, in *Cancer Theranostics*, Elsevier Inc., 2014, 285–325. doi: 10.1016/B978-0-12-407722-5.00017-7.

[21] A. Malaiya, D. Jain, and A. K. Yadav, in *Nano Drug Delivery Strategies for the Treatment of Cancers*, Elsevier, 2021, 145–164. doi: 10.1016/b978-0-12-819793-6.00007-2.

[22] M. Tagaya *et al.*, in *Key Engineering Materials*, Jan. 2013, 529–530, 1, 630–635. doi: 10.4028/www.scientific.net/KEM.529-530.630.

[23] Z. Liu *et al.*, *Drug Deliv.*, 16, 6, 341–347, (2009),

[24] Z. Akal, L. Alpsoy, and A. Baykal, *Appl. Surf. Sci.*, 378, 572–581, (2016),

[25] B. Wanjiku *et al.*, *Anal. Chem.*, 91, 11, 7208–7214, (2019),

[26] Y. Bi *et al.*, *Light Sci. Appl.*, 7, 1, (2018),

[27] T. Asai, H. Liu, Y. Ozeki, S. Sato, T. Hayashi, and H. Nakamura, *Appl. Phys. Express*, 12, 11, 112004, (2019),

[28] Z. Zhao *et al.*, *Nat. Commun.*, 12, 1, 1–12, (2021),

[29] C. Graf *et al.*, *Langmuir*, 34, 4, 1506–1519, (2018),

[30] C. Graf and E. Rühl, in *NanoScience and Technology*, Springer Verlag, 2019, 213–239. doi: 10.1007/978-3-030-12461-8_9.

[31] A. McLintock, C. A. Cunha-Matos, M. Zagnoni, O. R. Millington, and A. W. Wark, *ACS Nano*, 8, 8, 8600–8609, (2014),

[32] J. Wan, J. H. Wang, T. Liu, Z. Xie, X. F. Yu, and W. Li, *Sci. Rep.*, 5, (2015),

[33] T. S. Hauck, A. A. Ghazani, and W. C. W. Chan, *Small*, 4, 1, 153–159, (2008),

[34] I. Pastoriza-Santos, J. Pérez-Juste, and L. M. Liz-Marzán, *Chem. Mater.*, 18, 10, 2465–2467, (2006),

[35] *,†,§ Christina Graf, †,‡ Dirk L. J. Vossen, † and Arnout Imhof, and †,‡ Alfons van Blaaderen*, (2003),

[36] N. G. Bastús, F. Merkoçi, J. Piella, and V. Puntes, *Chem. Mater.*, 26, 9, 2836–2846, (2014),

[37] M. Tsuji *et al.*, *Cryst. Growth Des.*, 8, 7, 2528–2536, (2008),

[38] M. Lieber, J. Mazzetta, W. Nelson-Rees, M. Kaplan, and G. Todaro, *Int. J. Cancer*, 15, 5, 741–747, (1975),

[39] D. Cassano, M. Santi, F. D'Autilia, A. K. Mapanao, S. Luin, and V. Voliani, *Mater. Horizons*, 6, 3, 531–537, (2019),

[40] D. J. Frisch, M. J.; Trucks, G. W.; Schlegel, H. B.; Scuseria, G. E.; Robb, M. A.; Cheeseman, J. R.; Scalmani, G.; Barone, V.; Petersson, G. A.; Nakatsuji, H.; Li, X.; Caricato, M.; Marenich, A. V.; Bloino, J.; Janesko, B. G.; Gomperts, R.; Mennucci, B.; Hratch, "Gaussian 16." Gaussian, Inc., Wallingford CT, 2016.

[41] L.-K. Huy, W. Forst, and Z. Prášil, *Chem. Phys. Lett.*, 9, 5, 476–478, (1971),

[42] R. L. Jacobsen, R. D. Johnson, K. K. Irikura, and R. N. Kacker, (2013),

[43] L. Sun *et al.*, *Nano Lett.*, 7, 2, 351–356, (2007),

[44] L.-B. Zhao, R. Huang, Y.-F. Huang, D.-Y. Wu, B. Ren, and Z.-Q. Tian, *J. Chem. Phys.*, 135, 13, 134707, (2011),

[45] X. Ma *et al.*, *Sci. Rep.*, 6, 1, 1–12, (2016),

[46] Z. U. Akal, L. Alpsoy, and A. Baykal, *Ceram. Int.*, 42, 7, 9065–9072, (2016),

[47] M. Barella *et al.*, *ACS Nano*, (2020),

[48] M. Jacobs, A. Panneer Selvam, J. E. Craven, and S. Prasad, *J. Lab. Autom.*, 19, 6, 546–554, (2014),

[49] L. S. Nascimento, E. F. Macedo, J. A. Magalhães, L. R. M. Dona', and D. B. Tada, *MRS Adv.*, 1–9, (2020),

[50] A. F. Trindade *et al.*, *Org. Biomol. Chem.*, 12, 20, 3181–3190, (2014),

[51] A. R. Vortherms, R. P. Doyle, D. Gao, O. Debrah, and P. J. Sinko, *Nucleosides, Nucleotides and Nucleic Acids*, 27, 2, 173–185, (2008),

[52] Y. B. Patil, U. S. Toti, A. Khdair, L. Ma, and J. Panyam, *Biomaterials*, 30, 5, 859–866, (2009),

[53] "Carbon-13 nmr spectroscopy, high-resolution methods and applications in organic chemistry and biochemistry. Third Edition. By Eberhard Breitmaier and Wolfgang Voelter. VCH Pubs.: Weinheim, FRG. 1987. 515 pp. 24 × 18 cm. ISBN 0-89573-493-1. $135.00 - Byrn - 1987 - Journal of Pharmaceutical Sciences - Wiley Online Library." https://onlinelibrary.wiley.com/doi/abs/10.1002/jps.2600760918 (accessed Dec. 13, 2020).

[54] K. R. Jennings, *Org. Mass Spectrom.*, 26, 9, 813–813, (1991),

[55] F. M. Dayrit and A. C. de Dios, in *Spectroscopic Analyses - Developments and Applications*, InTech, 2017. doi: 10.5772/intechopen.71040.

7. Supplementary materials

7.1 Figures

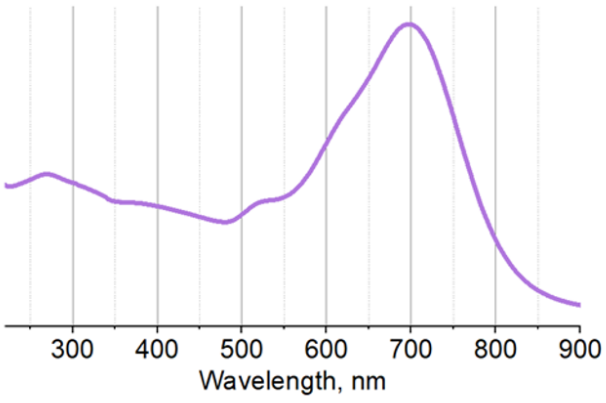

Cyanine 5.5 amine				
Experiment			Calculation	
Raman shift, cm^{-1}	Intensity, a.u		Raman, cm^{-1}	Assignment
727	**356**	vs	719	CC def
945	**344**	vs	956	CC str, CH def chain
1148	**175**	m	1156	CC str, CH def
1215	**94**	w	1178	CC str, CH def
1307	183	m	1309	CH def
1326	**211**	m	1328	CH def
1460	**239**	m	1460	NC-H3 def
1491	**162**	m	1498	CH def
1523	**171**	m	1544	CC str, CH def ring
1578	**96**	w	1544	CC str, CH def ring
1612	79	w	1619	central C=C str
1626	**113**	w	1634	central C=C str

Figure S1. Left: UV-vis absorbance spectra of unmodified CTAB-stabilized gold nanoparticles colloidal solution 10 times diluted (10.6 ug/ml). Right: assignment of the most pronounced Raman modes of AuNP@PSS@Cy5.5-NH2@PDDA@FA according to quantum chemical simulation of Cyanine 5.5 amine.

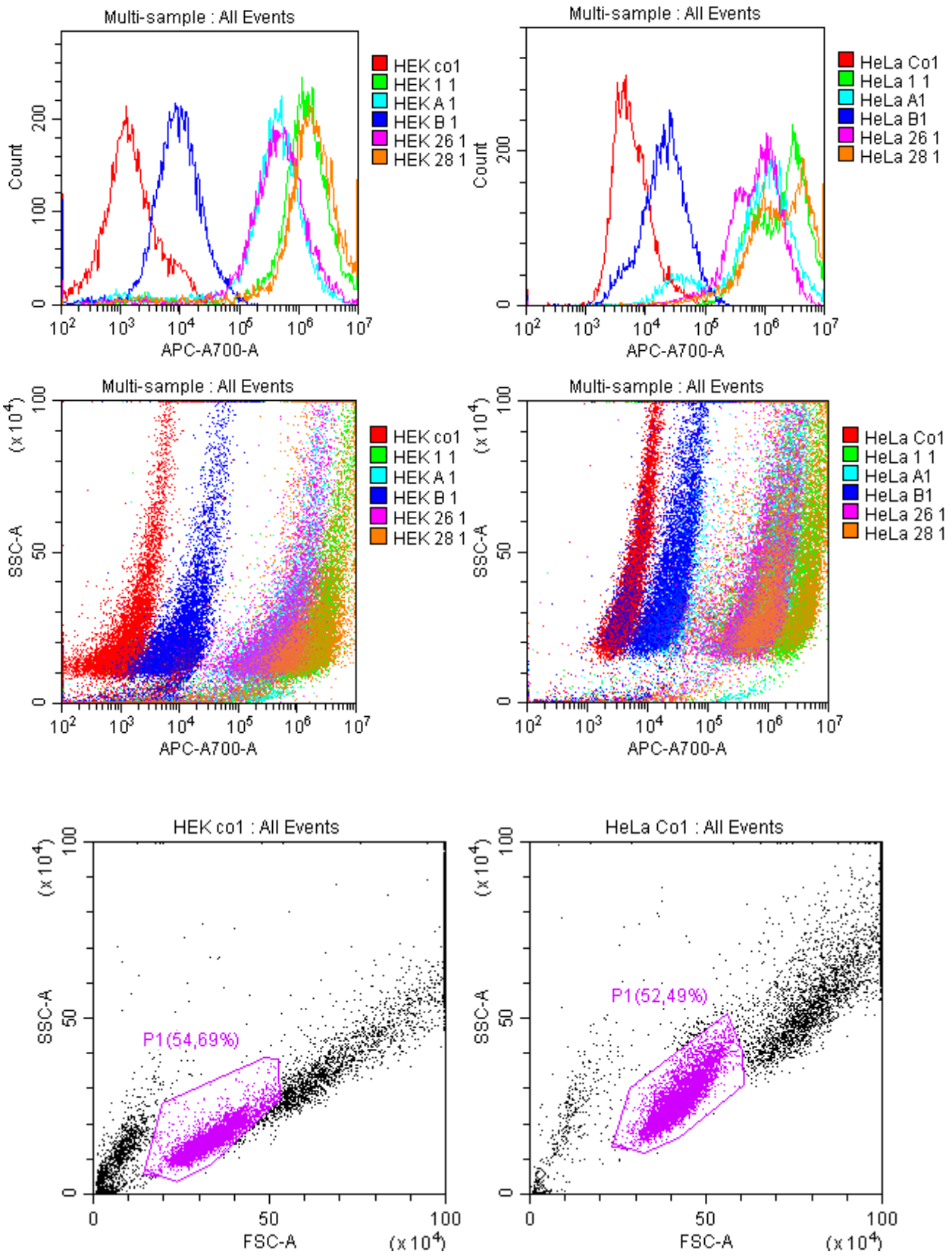

Figure S2. First row: histograms of the signal intensity distribution recorded at a wavelength of 712 nm and integrated over the registration window area of 25 nm, excitation line at 638 nm. Second row: An overlapping point representation of events for the same data. Third row: event selection based on side and forward violet light scatter (405 nm) from the cells (10000 events). Exposure time of nanoparticles: 24 hours.

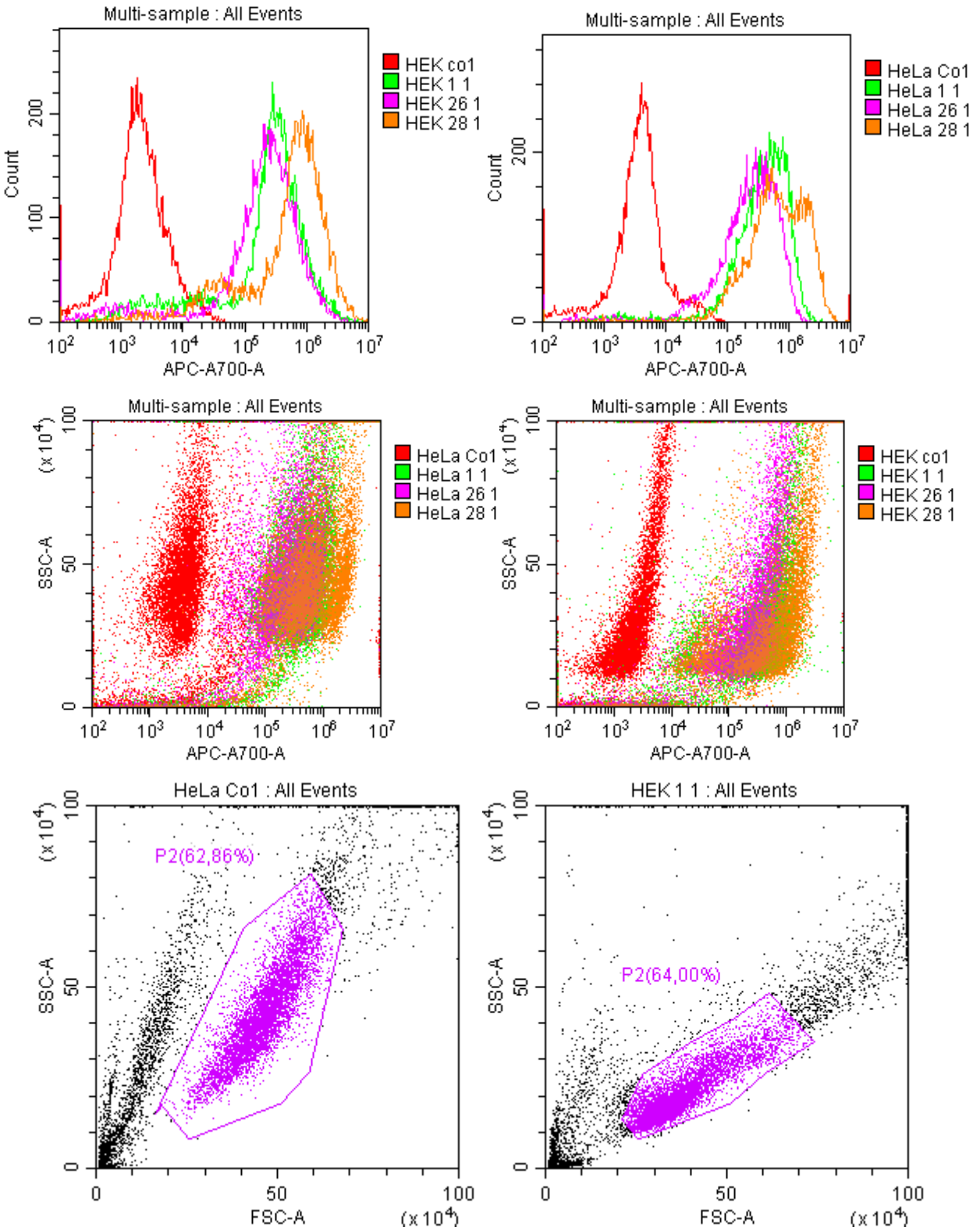

Figure S3. First row: histograms of the signal intensity distribution recorded at a wavelength of 712 nm and integrated over the registration window area of 25 nm, excitation line at 638 nm. Second row: An overlapping point representation of events for the same data. Third row: event selection based on side and forward violet light scatter (405 nm) from the cells (10000 events). Exposure time of nanoparticles: 2 hours.

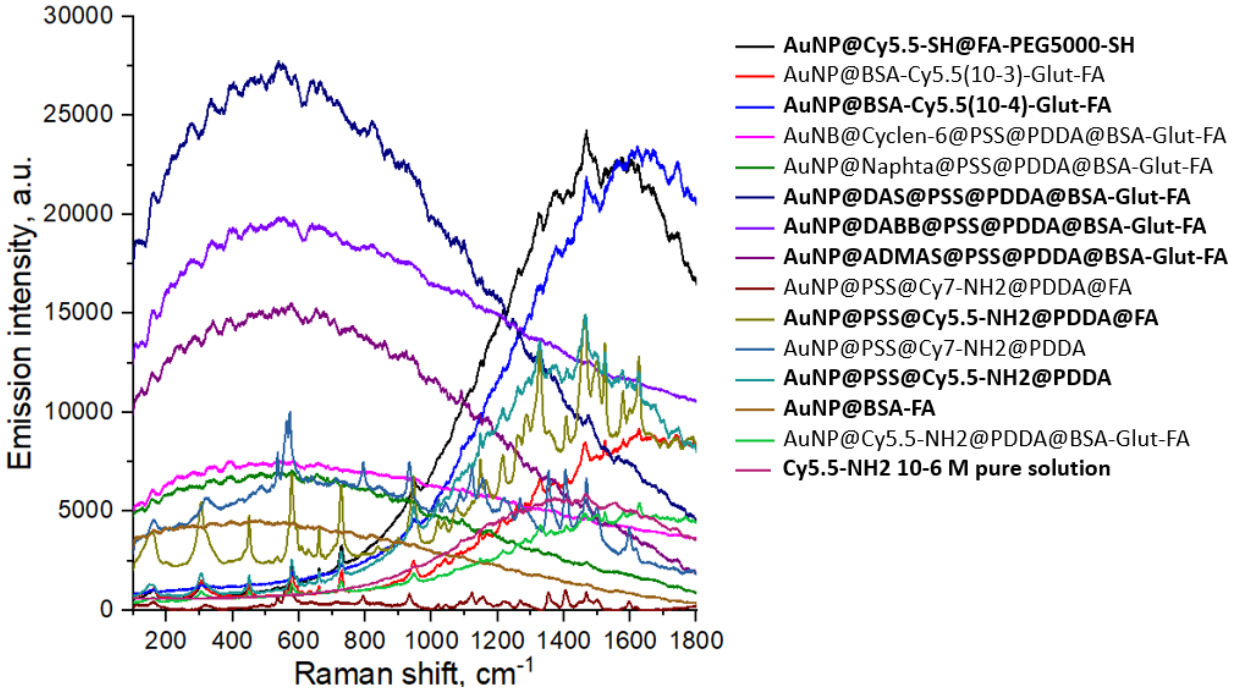

Figure S4. Surface Enhanced Raman Scattering and fluorescent signal of different nanoparticles under 632.8 nm excitation line

6.2 ^{13}C NMR of folic acid activated ether

In the first step, to improve the reactivity, the terminal carboxyl group of folic acid is activated by N-hydroxysuccinimide. Folic acid is poorly soluble in water (0.0016 g / 100 ml); therefore, the reaction is carried out in DMSO using 1,3-dicyclohexylcarbodiimide [50]. The method for the extraction of directly activated folic acid ester in its pure form has not been described in the literature, although references to such a step are found in at least two sources in which one can find the assignment of NMR chemical shifts, in other cases folic acid is conjugated directly to the final substrate, or added to excess without isolating ether from the reaction mixture смеси [22], [24], [46], [51], [52]. It is not possible to clearly prove the attachment of succinimide using proton shifts alone due to the absence of protons on the atoms that create the bond. However, the carbon atom at the terminal carboxyl group is capable of exhibiting a characteristic shift.

The by-product, dicyclohexylurea, precipitates and can be easily removed. For conjugation of folic acid to amino groups on the surface of nanoparticles, a water-soluble carbodiimide is preferred, because a water-soluble low-molecular-weight by-product can be easily removed later by dialysis or centrifugation.

According to the MestReNova modeling, during the formation of the folic acid ester in the 13C spectrum, peaks of identical carbon atoms are expected to appear at positions 27 ppm and 169 ppm, but this is not reliable evidence of bond formation, because the same peaks should also be present in the spectra of the mixture n -hydroxysuccinimide and folic acid. The characteristic criterion for the formation of ether is the shift of most carbon peaks towards higher ppm, and this is consistent with the experimental data:

^{13}C NMR of folic acid (101 MHz, DMSO): δ 174.38, 174.22, 166.87, 161.47, 154.21, 151.25, 149.09, 149.05, 148.78, 129.46, 128.42, 121.77, 121.54, 112.95, 111.65, 52.20, 46.38, 30.88, 26.47 ppm.

^{13}C NMR NHS-ester of folic acid (101 MHz, DMSO) δ 174.77, 174.59, 169.73 (succinimide), 166.46, 161.68, 154.59, 151.18, 148.97, 148.84, 148.60, 132.54, 129.28, 128.43, 122.95, 111.69, 52.69, 46.42, 45.92, 32.26 (succinimide), 31.45, 27.23 ppm.

The observed shift can be explained by the shift by the inductive acceptor effect of n-succinimide. Pulling off the electron density leads to a decrease in the screening of carbon atoms and an increase in the chemical shift [53]–[55].

8. Acknowledgments

The author is grateful to Prof. Dr. Burkhard Kleuser for support and access to the laboratory of the Institute of Pharmacy, Dr. Christian Gerke for help in maintaining cell lines and working on a flow cytometer, Steffen Thierbach for help in setting up optical experiments and a sense of humor, Tamasri Senapati for help in the experiment, scientific enthusiasm and pleasant company, Natalia Kolanovska for epoxy glue, without which it would be impossible to prepare cell samples for microscopy, Dr. Elena Solovyeva for her patience and Prof. Dr. Eckart Ruehl for making this all possible.

The research was carried out using the equipment of the SPbU "Optical and Laser Methods for the Study of Substances", "Methods for the Analysis of Composition of Substances", "Magnetic Resonance Research Methods", "Computing Center of St. Petersburg State University", "Nanotechnology" resource centers and equipment of the Free University of Berlin with the support of the German-Russian Interdisciplinary Science Center (G-RISC) funded by the German Federal Foreign Office via the German Academic Exchange Service (DAAD) (Funding Decision on Proposal: A-2021 a-2 r).

9. Personal Impressions

Student scientific exchange pursues not only individual scientific goals, but helps to establish contacts and expand the perception of the world. For many, this is the first experience of scientific work in a foreign university - for whom the first experience of a principled independent life abroad. For me personally, the experience gained in a month is comparable to a year at the home university: I was given the opportunity to completely independently plan the experiment - from the choice of cell lines for the experiment and ending with the choice of wave numbers for an optical experiment. I met the lively and active support of my German colleagues, moreover, I was allowed not only to work on optical equipment, but also to carry out preparatory cell work. This forces one to "grow up" as a researcher, to take responsibility for one's own decisions and mistakes. However, this should not be feared - the exchange program does not have any strict high requirements for the result, and the scientific leadership is always ready to help. Therefore, it is difficult to overestimate how important participation in such projects is for a person who is going to connect his life with science.


Freie Universität Berlin
Arnimallee 22
FU
FB Biologie, Chemie, Pharmazie
Fachbereichsverwaltung
FB Biologie, Chemie, Pharmazie
Institut für Chemie und Biochemie
Physikalische und Theoretische
Chemie
FB Biologie, Chemie, Pharmazie
Institut für Chemie und Biochemie
Organische Chemie